NON-SILICA MICROSTRUCTURED OPTICAL FIBERS

T.M. Monro, H. Ebendorff-Heidepriem, X. Feng
Optoelectronics Research Centre
University of Southampton
Southampton SO171BJ, United Kingdom

ABSTRACT

Microstructured fibres offer a range of optical properties that cannot be achieved in conventional (solid) optical fibres. Although to date, most work in this field has focused on silica glass, non-silica microstructured fibres are attractive for applications including nonlinear devices, mid-IR transmission and photonic bandgap operation. A review of progress in the development and applications of non-silica microstructured fibres will be presented.

INTRODUCTION

Research in the field of microstructured optical fibers has progressed rapidly in recent years because these fibres can offer a diverse range of novel optical properties that cannot be provided by more conventional optical fibers, which opens up diverse potential applications in telecommunications, industrial processing, metrology, medicine and beyond. The transverse cross section of a microstructured fiber typically contains an approximately periodic arrangement of air holes that run along the fiber length. The vast majority of microstructured fibers that have been produced to date are air/silica fibers that contain an arrangement of air holes embedded in undoped silica glass [1-4].

The holes within the microstructured fibers act as the fiber cladding, and light can be guided using two quite different mechanisms. *Index-guiding* microstructured fibers guide light due to the principle of modified total internal reflection, and such fibers are widely known as holey fibers (HFs) [2]. In this class of fibers, the holes effectively act to lower the effective refractive index in the cladding region, and so light is confined within the solid core, which has a relatively higher refractive index. This guidance mechanism does not reply on the use of a periodic arrangement of holes [5]. However, since in practice silica holey fibers are generally made by stacking a large number of circular capillaries, the resulting air holes are typically arranged on a hexagonal lattice, and so these fibers are also often referred to as photonic crystal fibers [3].

Index-guiding holey fibers exhibit novel optical properties for two principal reasons: (1) the effective refractive index of the holey cladding region can vary strongly as a function of the wavelength of light guided by the fiber and (2) the air/glass features provide a large refractive index contrast. In addition, the optical properties of index-guiding HFs are determined by the configuration of air holes used to form the cladding, and many different arrangements can be envisaged within this flexible fiber geometry. For these reasons, it is possible to design single material silica fibers with properties that are not possible in conventional fibers such as broadband single-mode guidance [6] or anomalous dispersion in single mode fibers at wavelengths down to 560nm [7]. Simply by scaling the dimensions of the features within the fiber profile, pure silica HFs can have mode areas ranging over three orders of magnitude. At one extreme, HFs with large mode area are of great promise for high power transmission systems (see for example [8], [9]). At the opposite end of the scale, by

combining small-scale cladding features with the large effective index contrast possible in HFs, it is possible to achieve tight mode confinement, and thus high effective fiber nonlinearities can be obtained. Such fibers have been used in a variety of nonlinear devices including devices for wavelength conversion, supercontinuum generation, all-optical switching and data regeneration, pulse compression and soliton formation (see for example [10]-[21]).

Photonic bandgap microstructured fibers (PBGFs) can guide light by an alternative guidance mechanism, the so called photonic bandgap effect, if the air holes that define the cladding are arranged on a periodic lattice [4]. By suitably breaking the periodicity of the cladding it is possible to introduce a localized mode within this defect. Such a defect can act as a core, and guide light within well-defined frequency windows. Hollow core photonic bandgap fibers can be designed to transmit at near-infrared wavelengths and are of particular interest for gas/light interactions and the transport of high intensity optical fields.

In the single-material holey and photonic bandgap fibers described thus far, light is solely confined by the holes in the cladding. Hybrid microstructured fibers are another class of fiber that combines a high-index doped core with a holey cladding. At one extreme, in *hole-assisted fibers*, light is guided by the relatively higher index of the doped core, and the air holes located in the cladding of a conventional solid fiber act to subtly modify properties such as dispersion [22]. In air-clad fibers, an outer cladding with a high air-filling fraction creates a high numerical aperture inner cladding which allows the realization of cladding-pumped high power lasers [23]. Alternatively, dopants can be added to the core of a HF to create novel HF-based amplifiers and lasers (see for example [24]).

Most work to date in the field of microstructured fibers has focused on silica glass technology, which allows the definition of a diverse range of high quality transverse fiber cross-sections via the capillary stacking fabrication technique. This field has now begun to come of age. Advances in fiber fabrication techniques have reduced the losses of both fiber types dramatically in recent years (to 0.3dB/km for HFs [25] and 1.7dB/km for PBGFs [26]). The prospect of microstructured silica fibers with a lower transmission loss than conventional fibers represents a tantalizing possibility with the potential to revolutionize telecommunications.

The combination of the microstructured fiber concept with non-silica glasses is a relatively unexplored field which promises the development of a host of new fibers and operational regimes not achievable in existing fibers. For example, recently compound glasses with high intrinsic optical nonlinearity (such as lead-silicate, tellurite and bismuth-oxide) have been used to produce HFs with extreme values of effective fiber nonlinearity [27]-[34]. In addition, polymer-based HFs have been reported [35]. A number of non-silica glasses transmit at wavelengths substantially beyond silica into the mid-IR (for example chalcogenide glasses), and microstructured fibers made from such materials promise a new means of providing power delivery at these wavelengths. Note that in contrast to conventional fibers, microstructured fibers can be made from a single material, which eliminates the problems induced by the requirement that the core/cladding glasses are thermally and chemically matched. This opens up the prospect of using microstructured fiber technology as a tool for realizing optical fibers from an extremely broad range of optical materials.

Other classes of microstructured fiber have also begun to emerge. In particular, microstructured fibers with solid cladding designs have recently been demonstrated. In these fibers, low index glass inclusions are embedded in a higher-index glass matrix either in the form of circular inclusions [36]

or in nested layers [37]. These fibers combine the practicality of a solid cladding with the design flexibility provided by the transverse microstructure.

The aim of this paper is to provide an overview of the progress to date and range of potential applications for non-silica microstructured optical fibers. We begin by reviewing the fabrication techniques that have been employed to make non-silica microstructured fibers.

FABRICATION APPROACHES

Preform Fabrication

As noted above, the vast majority of microstructured fibers that have been produced to date have been made from silica glass, and the preforms for these fibers are usually fabricated using stacking techniques. Capillary tubes are stacked in a hexagonal configuration, and the central capillary can then be replaced with a solid glass rod, which ultimately forms the fiber core. The stacking procedure is flexible: for example active fibers can be made using rare-earth-doped core rods, off-center or multiple core fibers can be readily made by replacing a non-central or multiple capillaries, etc. The reproducibility of the structured profile in the preform depends on having long uniform capillaries to stack and achieving a good stack with many tubes. One significant drawback of the stacking approach is that the preform fabrication is labor-intensive.

Recently, attention has focused on the fabrication of microstructured fibers in a range of non-silica glasses. In general, such compound glasses have low softening temperatures relative to silica glass, which allows new techniques to be used for the fabrication of structured preforms such as rotational casting and extrusion. The technique that has been used for the majority of non-silica microstructured fibers made thus far is extrusion [27-34]. In this process, a glass billet is forced through a die at elevated temperatures near the softening point, whereby the die orifice determines the preform geometry. Once the optimum die geometry and process parameters have been established, the preform fabrication process can be automated. In this way good reproducibility in the preform geometry has been achieved [32]. One advantage of the extrusion technique is that the preform for the microstructured part of a fiber can be produced in one step. In addition, extrusion allows access to a more diverse range of cladding structures, since the holes are not restricted to hexagonal arrangements.

Fiber Fabrication

To produce fibers with relatively large scale features, fibers are in general drawn directly in a single step from the preform. For small scale features, the preform is first reduced to a cane of 1-2mm diameter on a drawing tower, and in a second step this cane is inserted in a solid jacketing tube and then drawn to the final fiber. One of the most challenging aspects of air/glass microstructured fiber fabrication is to prevent collapse of the holes and to achieve the target hole size and shape during caning and fiber drawing. The microstructured profile can be affected by the pressure inside the holes, surface tension of the glass and temperature gradient in the preform. Note that compared with silica glass, most non-silica glasses have significantly steeper viscosity curves, which leads to greater demands on the process control during fiber drawing. Nevertheless, a high degree in the reproducibility of the HF geometry has already been demonstrated for both lead silicate glass [32] and bismuth glass [33,34].

HIGH NONLINEARITY FIBERS

Design Concept

Microstructured fiber technology has enabled significant progress in the development of fibers with high effective nonlinearity. This is achieved by combining a small core design with a high numerical aperture (NA) to yield tight mode confinement. One common measure of fibre nonlinearity is the effective nonlinearity γ [38]: $\gamma = 2\pi n_2 / (\lambda A_{eff})$, where n_2 is the nonlinear coefficient of the material, λ the wavelength and A_{eff} is the effective mode area.

Pure silica holey fibers with effective mode areas as small as 1.3 μm^2 have successfully been fabricated, exhibiting effective nonlinearity coefficients as high as 70 $W^{-1}km^{-1}$ at 1550 nm [39], i.e. around 70 times more nonlinear than standard single mode fibers. This value represents the theoretical limit in nonlinearity that can be achieved in a silica/air fiber. However, the material nonlinearity of compound glasses [40] can be more than one order of magnitude larger than that of silica [38]. The combination of highly nonlinear glass composition and small core/high NA HF geometry allows a further dramatic increase of the fiber nonlinearity.

As an example, we estimate the magnitude of the nonlinearity that could ultimately be achieved in a bismuth oxide glass holey fiber by considering the case of a rod of glass suspended in air (see description of bismuth glass to follow). This simplified geometry represents the fundamental limit in the mode area/nonlinearity that can be achieved in an air/glass microstructured fiber made from this material. The highest nonlinearity of γ=2200 W^{-1} km^{-1} is obtained when the core rod is ~0.8 μm in diameter (Figure 1). Note that this nonlinearity is a factor of two higher than the record nonlinearity achieved thus far for a chalcogenide glass fiber with conventional solid cladding [41].

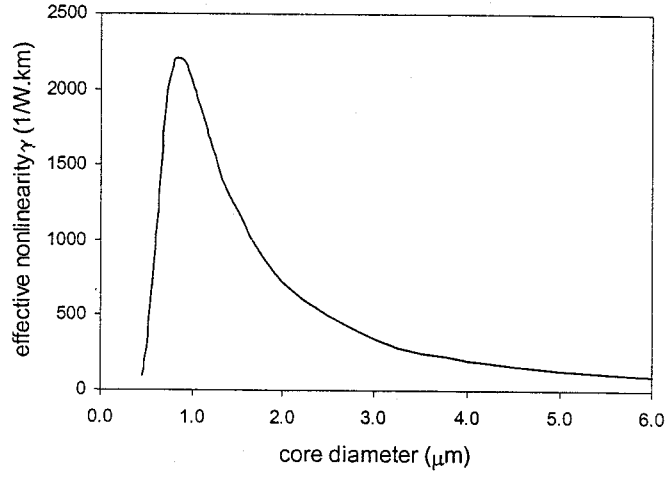

Figure 1. Calculated nonlinearity (γ) for an air-suspended rod of bismuth oxide glass

Here we review fabrication techniques that have been used to make these fibers, the range of glasses that have thus far been successfully used, and some key results that have been obtained using nonlinear non-silica holey fibers.

Fabrication Approach

All of the small-core non-silica microstructured fibers produced to date have exploited extrusion techniques to fabricate structured fiber preforms with mm-scale features from bulk glass billets. As an example, consider the structured preform shown in Figure 2(a). In this geometry, the core (center) is attached to three long fine supporting struts. The outer diameter of this preform is approximately 16mm. The preform was reduced in scale on a fiber drawing tower to a cane of approximately 1.7mm diameter (Figure 2(b)).In the last step, the cane was inserted within an extruded jacket tube, and this assembly was drawn to the final fiber (Fig.1(c)). The illustrative examples shown in figures 2 (a)-(c) are made from the lead silicate glass SF57, and are taken from Reference [32]. This procedure has also been used to make nonlinear fibers from other materials including bismuth glass (for more detail see below). A similar technique has been used to produce small-core tellurite microstructured fibers in which the core is supported by six long fine struts [29]. In Ref [29], the preform extrusion is performed directly on a fiber drawing tower, which allows the preform to be reduced to ≈1mm diameter cane directly at the time of extrusion.

The core diameter can be adjusted during fiber drawing by an appropriate choice of the external fiber diameter. Small core dimensions are chosen to provide tight mode confinement and thus high effective nonlinearity. For fiber designs of the type shown shown in figure 2, core diameters in the range 1.7-2.3 μm correspond to struts that are typically >5 μm long and <250 nm thick. These long, thin struts act to isolate the core optically from the external environment, and thus ensure that confinement loss is negligible [42]. Note that these fibers have an improved structure when compared with the earliest fibers of this type that were made [27]. Excellent structural reproducibility has been demonstrated using this fabrication technique [32]. Next, we review the glasses in which nonlinear microstructured fibers have successfully been fabricated to date.

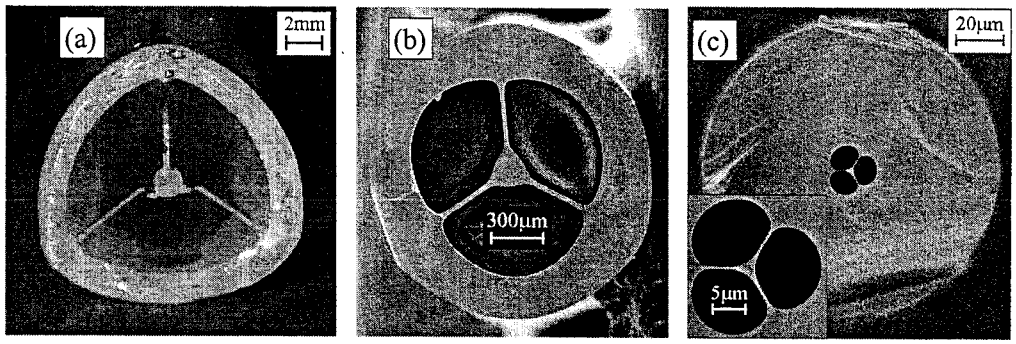

Figure 2: (a) Cross section through extruded preform, (b) SEM image of cane cross section, (c) SEM image of holey fiber cross section.

SF57: Lead silicate glasses are a promising host material for highly nonlinear HFs. Although their intrinsic material nonlinearity (and indeed linear refractive index) is lower than chalcogenide and heavy metal oxide glasses [43], they offer higher thermal and crystallization stability and less steep viscosity-temperature-curves, while exhibiting low softening temperatures [44]. Among

commercially available lead silicate glasses, the Schott glass SF57 exhibits the highest nonlinearity. The softening temperature of SF57 is 520 °C [45], the nonlinear refractive index of this glass was measured to be 4.1×10^{-19} m^2/W at1060 nm [40], and the linear refractive index of SF57 is ≈1.8 at 1550 nm [45]. The zero-dispersion wavelength for the glass is 1970 nm and the material dispersion is strongly normal at 1550 nm. Compared with chalcogenide and heavy metal oxide glasses (n~2.4 at 1550 nm), the significantly lower refractive index of SF57 should enable more efficient integration with conventional fiber systems.

Bismuth: Bismuth oxide-based glass is an attractive novel material for nonlinear devices. It shows high nonlinearity but without containing toxic elements such as Pb, As, Se, Te [46]. Moreover, the bismuth-based glass exhibits good mechanical, chemical and thermal stability, which allows easy fiber fabrication process. A nonlinear fiber [47] and a short Er-doped fiber amplifier with broadband emission [48] have been developed from this glass. In addition, bismuth-oxide-based fibers can be fusion-spliced to silica a fiber [49], which offers easy integration to silica-based networks. The fibers review in this paper were made from bismuth-oxide-based glass developed at Asahi Glass Company. Due to the high bismuth content, the glass exhibits a high linear and nonlinear refractive index of n=2.02 and $n_2=3.2\times10^{-19}$ m^2/W at 1550 nm, respectively [47], and this glass has a softening temperature of 550 °C.

Tellurite: Tellurite glasses, like lead silicate and bismuth glasses, offer high refractive index and high optical nonlinearity ($n_2=2.5\times10^{-19}$ m^2/W) [29]. In addition, tellurite glass has good infrared transmittance and has a low phonon energy relative to other oxide glasses [50]. Furthermore, tellurite glasses are more stable than fluoride glasses, have higher rare-earth solubilities than chalcogenide glasses [50] and have an order of magnitude larger Raman gain peak than fused silica [51]. Tellurite glasses have a low softening temperature around 350 °C [50].

High nonlinearity microstructured fibres: Key results to date

- SF57 holey fiber with an effective nonlinearity coefficient of $\gamma=640W^{-1}km^{-1}$ (loss≈2.6dB/m at 1550nm) [31]
- Anomalous dispersion at 1550nm and Raman soliton generation in SF57 holey fiber [31]
- Observation of the soliton self frequency shift and pulse compression in SF57 holey fiber [31]
- Tellurite holey fiber with $\gamma=48W^{-1}km^{-1}$ (loss ≈5dB/m at 1550nm) [29]
- Observation of first and second order Stokes stimulated Raman scattering in 1m of tellurite holey fiber [29]
- Bismuth-oxide-based glass holey fiber with $\gamma=460$ W^{-1} km^{-1} [33]
- Demonstration of splicing of bismuth holey fibers to conventional fibers [34]
- Demonstration of supercontinuum generation in SF6 holey fiber [28]

Discussion:

Both the effective fiber nonlinearity and effective fiber length determine the performance of a nonlinear device (the effective length depends on the propagation loss). Small-core high-NA holey fibers based on bismuth-oxide and lead-silicate glasses have clearly higher fiber nonlinearity but also higher propagation loss compared with highly nonlinear silica holey fibers. However, for short devices using ≤1 m fibre length, fibre losses of ≤2 dB/m can be readily tolerated. For ≤2 dB/m, the effective fibre length is ≥80% of the real fibre length of ≤1 m, whereas the nonlinearity of non-silica fibres can be up to 10 times higher than that of silica holey fibres. In other words, in compact devices using ≤1 m fibre length with ≤2 dB/m loss, the increase in fibre nonlinearity obtained by using nonlinear glass compositions clearly outweighs the decrease of the effective fibre length due to higher propagation losses. Thus, provided that relatively low loss fibers can be produced, highly nonlinear compound glass holey fibres can exhibit a better nonlinear performance (lower power or shorter fibre length requirement) compared with nonlinear silica holey fibers.

Most nonlinear/high-index glasses have a high normal material dispersion at 1550 nm, which tends to dominate the overall dispersion of fibers with a conventional solid cladding structure. However, for many nonlinear device applications, anomalous or near-zero dispersion is required. Fortunately, the cladding geometry significantly affects the waveguide dispersion, allowing the highly normal material dispersion to be overcome. Indeed, for example, lead silicate holey fibers showing anomalous dispersion at 1550 nm have been demonstrated [32]. The fact that fiber dispersion is anomalous also enables us to exploit soliton effects [31].

To make practical fiber-connectorized devices, splicing of compound glass holey fibers to silica fibers is important. Recently, bismuth-oxide based holey fiber with $A_{eff} \sim 2.8\ \mu m^2$ has been spliced to a silica SMF28 patchcord using a conventional mechanical cleaver and fusion splicer [34]. To reduce the overall mode-mismatch loss, two intermediate buffer stages were used. The bismuth glass holey fiber itself was spliced to a silica fiber with $A_{eff} \approx 14 \mu m^2$. Due to the much lower melting temperature of the bismuth glass relative to silica glass, very small values for the fusion time and current were used. The splices achieved were mechanically strong, especially with respect to applied strain in the axial direction (Figure 3a). Although the total splicing losses achieved to date are still quite high (5.8 dB) – they can largely be accounted for by individual mode-mismatches at the various buffer fiber interfaces (minimum 3.8 dB, without taking into account the mismatch in the mode shape) and an additional 0.1 dB due to Fresnel reflection at the bismuth glass HF / silica fiber interface. There is considerable scope for reducing the Fresnel reflections using accurately controlled angle cleaves at the bismuth glass /silica fiber splice. The introduction of an additional silica HF based buffer stage should help to considerably further reduce the mode-mismatch. Splicing of bismuth glass holey fiber to silica fiber has resulted in two benefits in the fiber performance. One is the reduction of coupling losses between the two fibers by 0.9 dB relative to butt coupling. The other is the achievement of robust single-mode guidance in the bismuth glass holey fiber at 1550 nm, although the fiber can support more than one mode in case of free-space coupling. An IR image of the far end of the connectorized holey fiber, when laser pulses at 1558 nm were launched into the fibre, showed that only the fundamental mode was excited (Figure 3b). (The image also demonstrates

that the fundamental mode of the holey fiber has a triangular mode shape, in agreement with the predicted mode profile [33].)

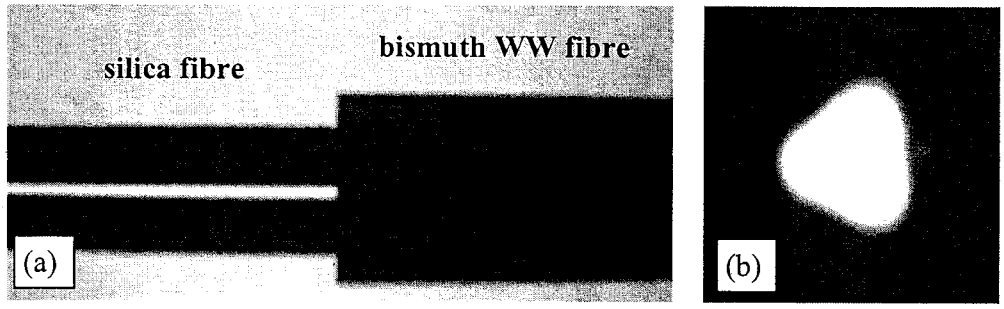

Figure 3 (a) Microscope image of bismuth glass holey fiber to silica fiber splice, (b) IR image of the near-field pattern of the connectorized holey fiber.

NEW TRANSMISSION FIBERS

A range of non-silica glasses can exhibit properties such as transparency in the mid-IR region and high solubility of rare-earth ions that are not available in silica glass and hence non-silica HFs are of particular promise for applications in mid-IR region and active devices. One challenge for high power applications in compound glass-based fibers is the onset of intensity-dependent nonlinear effects. The use of single-mode HF large-mode-area (LMA) designs [8] is one means of minimizing such nonlinear effects. Since the nonlinear refractive index (n_2) of non-silica glasses is typically in the range $(1\text{-}50)\times10^{-19}m^2/W$, higher than that of silica glass (2.7×10^{-20} m^2/W) by 1-2 orders of magnitude, very large-mode-areas ($>>100\mu m^2$) are required to reduce the effective nonlinearity γ to below $60W^{-1}km^{-1}$. In practice, it is challenging to fabricate compound glass LMA HFs with the complex microstructured cladding structures required to provide low NA guidance (i.e. a large number of relatively small air holes). Here we review recent work on the development of large mode area single mode lead silicate holey fiber.

A holey fiber with a mode area of $40\mu m^2$ at 800nm was fabricated from the Schott lead silicate glass SF6 using the conventional capillary-stacking technique (previous only used successfully for the fabrication of silica HFs). The cross-sectional microstructure of this HF is shown in Figure 4 (a) & (b), where a four-ring microstructured cladding can be seen. The hole-to-hole spacing Λ in the hexagonally arrayed holey cladding was measured to be 4.3μm. In addition to the principal holes with an inner-diameter (ID) of 2.7μm (d_1), six smaller holes with an ID of 0.3μm (d_2) are periodically distributed in the second ring surrounding the solid core. For the holes near the solid core, i.e., the holes with sizes d_1 and d_2, the ratio of hole-diameter to the hole-to-hole spacing Λ is $d_1/\Lambda=0.63$, and $d_2/\Lambda=0.07$, respectively. The 5.5μm (d_3) holes only weakly influence the optical guidance properties of this HF as they are located far from the core. Robust single mode guidance, from at least 700 to 800nm was observed in this HF. The effective mode area of the fundamental mode $A_{eff}=40\mu m^2$ was extracted from the measured mode intensity profile. Although this value of mode area is still not large enough to avoid intensity-dependent nonlinear effects in this SF6-based HF, this work demonstrates that the capillary-stacking technique can be successfully demonstrated to

fabricate soft-glass HFs with complex holey cladding. We anticipate that high-index glass based single-mode HF with very large mode areas (>>100μm^2) should be possible using this technique in the future.

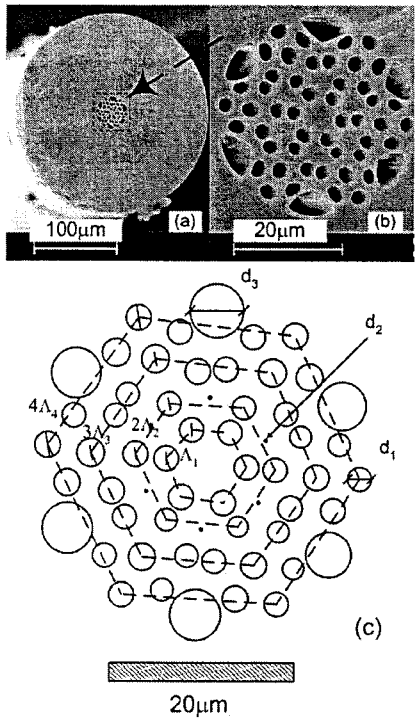

Figure 4 (left) SEM (Scanning Electron Microscope) photographs of SF6 glass holey fibre.

SOLID MICROSTRUCTURED FIBERS

Motivation

Research to date on silica microstructured fibers has shown that the combination of wavelength-scale features and a large refractive index contrast is a powerful means of obtaining fibers with a broad range of useful optical properties. However, there are some practical drawbacks associated with the use of air/glass fibers. When compared with solid fibers, air/glass microstructured fibers are challenging to splice, polish, taper, and, when the cross-section is largely comprised of air, they can be fragile. In addition, it can be challenging to fabricate kilometer-scale holey fibers with identical and controllable cladding configurations. This is because the transverse profile of a drawn microstructured fiber is sensitive to the effect of pressure inside the holes, surface tension at the air/glass boundaries and temperature gradients present during the fiber drawing process. To prevent the collapse of the holey microstructure in HFs, the holes within the preform are often sealed, and consequently the air pressure inside the structure increases during fiber drawing because of the decrease of the air volume remaining in the preform. Hence the dimensions of the microstructured cladding are often time-dependent as well as dimension-dependent. Note that the optical

characteristics of microstructured fibers can be sensitive to the cladding configuration and even minor changes in the microstructure can cause noticeable deviations in properties such as dispersion.

The development of microstructured fibers with solid microstructured claddings promises to eliminate these drawbacks. Two different implementations of this concept have recently been realized. The first approach is to replace the air holes in the transverse structure of an air/glass microstructured preform with low index glass regions to produce an index-guiding solid holey fiber [36]. Another approach is to form a fiber in which the cladding is defined by a series of thin nested layers of glass (a Bragg-type fiber cladding) to form an air-guiding fiber [37]. In both approaches, the basic requirement is the identification materials which are thermally and chemically matched in order that they can be drawn into optical fiber and which provide a sufficient index contrast to allow light to be confined either by index-guiding or photonic bandgap effects without requiring unfeasibly large numbers of cladding features. Note that while this approach may have some practical advantages, as suggested above, it clearly restricts the range of materials that can be used.

Solid Holey Fiber

Here we review the recent development of all-solid index-guiding holey (SOHO) fiber based on two thermally-matched silicate glasses with a high index contrast (as described in Reference [36]).

Fabrication: A borosilicate glass containing lead-oxide (PbO >30mol.%) with a refractive index of n=1.76 at 1.55μm, was selected as the background material (labeled B1 thereafter) for this SOHO fiber. Another silicate glass containing high alkali-oxide (Na_2O, K_2O etc) with index n=1.53 at 1.55μm was selected as the material to fill in the holes (H1). These glasses were selected because of their mechanical, rheological, thermo-dynamic and chemical compatibility. Rods of H1 glass were inserted into B1 tubes, both of which were drilled from bulk glass samples. These rod/tube structures were caned on a fiber drawing tower and stacked around a core rod of B1 glass within a B1 glass jacket tube using the capillary-stacking technique that is used to produce silica HFs. This structured preform was then drawn using a two-stage drawing procedure to produce two fibers: one with an outer diameter (OD) of 440μm and the other with an OD of 220μm.

Configuration of solid-microstructured cladding: Figure 5 shows cross-sectional profiles of the 220μm OD fiber taken using a Scanning Electron Microscope (SEM). From Figures 5 (a) & (b), it can be seen that this SOHO fiber is indeed an all-solid fiber without any observable air holes. However when the accelerating voltage (EHT) of the SEM is increased from 2.72kV to 22.00 kV, the microstructure in the cladding region becomes apparent. This occurs because the backscattering coefficient of the primary electrons from the SEM is a monotonically increasing function of the atomic number [52]. As a result, glasses with low average atomic number and consequently with the low density exhibit relatively lower brightness than materials with high density. Thus, as shown in Figures 5(c) and (d), the large density difference between B1 and H1 glasses (5.2 g/cm^3 and 2.9 g/cm^3 respectively) it is possible to distinguish the distribution of each material within the fiber profile.

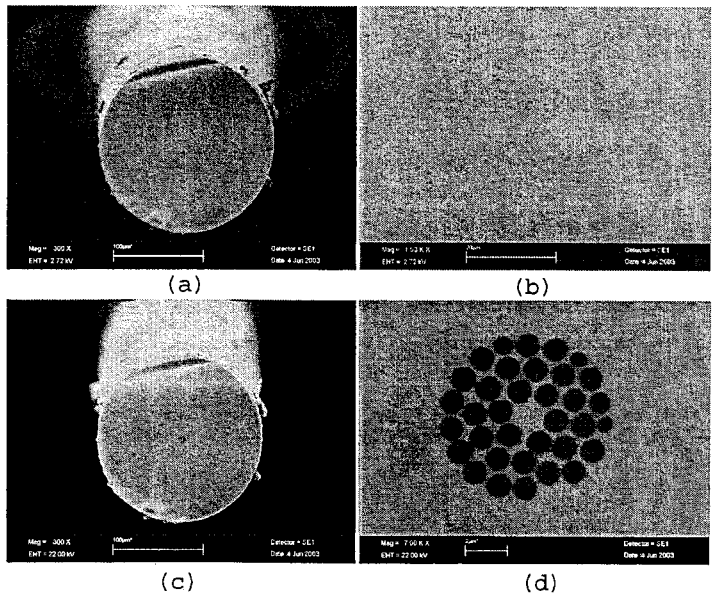

Figure 5: SEMs of 220μm diameter SOHO fiber by adjusting accelerating voltage (EHT) (a) whole view, EHT = 2.72 kV, (b) zoomed center view, EHT = 2.72 kV; (c) whole view, EHT = 22.00 kV, (d) zoomed center view, EHT = 22.00 kV

Typically when air/glass holey fibers are drawn, the holes become non-circular due to surface tension effects, which modify the geometry of the cladding. Hence the details of the resulting cross-sectional profiles depend on the draw-down ratio, and this becomes particularly apparent when small-scale features are required. Since the optical properties of such fibers can be sensitive to the cladding configuration, this effect can make it difficult to predetermine the preform required for a given fiber specification. Figure 6 compares the all-solid claddings of the 1mm cane, 440μm fiber and 220μm fiber. First, note that all the low index (black) regions retain their circularity, regardless of the draw-down ratio. Second, the d/Λ ratio (d: average diameter of the low index regions, Λ: the pitch (center to center spacing) of these regions) is ~0.81 regardless of the fiber OD. SOHO fibers thus provide a practical way of avoiding structural deformations during fiber drawing.

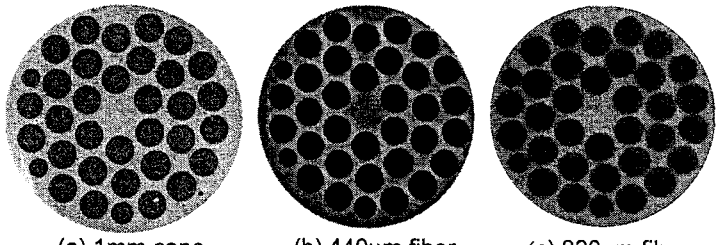

Figure 6. SEMs of microstructured cladding in (a) 1mm cane inserted into jacket tube before drawing, (b) 440μm OD fiber with Λ=4μm and (c) 220μm OD fiber with Λ=2μm. (EHT = 22 kV)

Fiber attenuation: The index contrast of B1/H1 SOHO fiber is $\Delta n = 0.23$ at 1.55μm, less than that in silica/air HF ($\Delta n = 0.44$ at 1.55μm), which might at first sight be expected to result in poorer mode confinement. However, the refractive index of the background glass, H1 (n=1.76 at 1.55μm) is higher than that of silica (n=1.44 at 1.55μm) which might be expected to lead to improved mode confinement. To resolve which factor dominates, Figure 7(a) shows the calculated confinement losses of the fundamental mode in a range of B1/H1 based SOHO fibers. These predictions were made with the multipole technique [53], which can model the properties of fibers with circular holes, so it is particularly well suited to this SOHO fiber. Note that the material absorption and the fabrication defects have been ignored and it is assumed that the holes lie on a hexagonal lattice. It can be seen that when $\Lambda = 4\mu m$, the confinement losses decrease rapidly to less than 0.001 dB/m by (1) increasing d/Λ ratio from 0.5 to 0.8 or more, or (2) by increasing the number of the rings from 2 to 4 or more with a fixed $d/\Lambda = 0.5$. Figure 7(a) indicates that is possible to design B1/H1 SOHO fibers (when $\Lambda = 4\mu m$) with negligible confinement loss provided that the d/Λ ratio is sufficiently large (0.8 or larger), as is the case for our 440μm OD SOHO fiber.

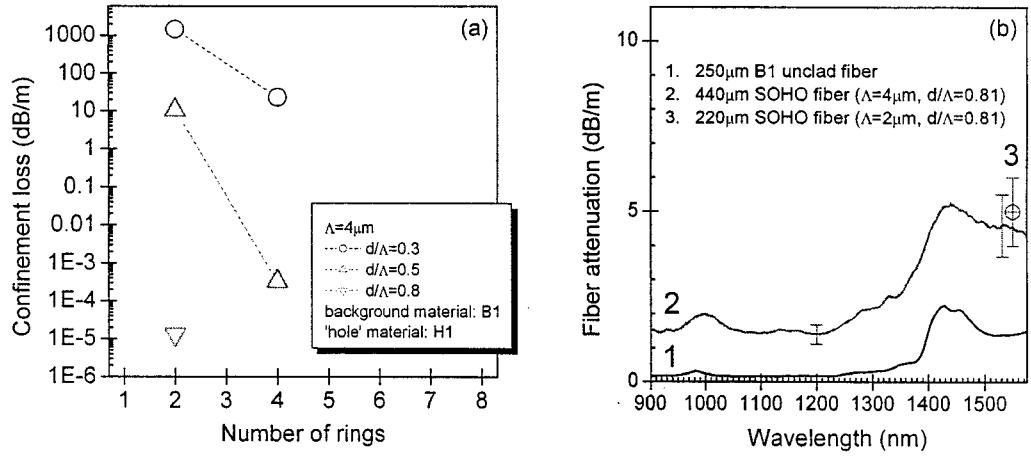

Figure 7(a) Calculated confinement losses of B1/H1 based SOHO fiber as a function of the number of hexagonal packed rings and their diameter to spacing ratio d/Λ with $\Lambda = 4\mu m$ at 1.55μm; (b) measured propagation attenuation of (1) unclad 250μm B1 fiber, (2) 440μm B1/H1 SOHO fiber, (3) 220μm B1/H1 SOHO fiber. Note that (3) is a spot measurement at 1550nm. Measurement errors are plotted.

Figure 7(b) shows the measured fiber attenuation for the case of a 250μm unclad/unstructured B1 fiber, 440μm B1/H1 SOHO fiber with $\Lambda = 4\mu m$ and $d/\Lambda = 0.81$, and 220μm B1/H1 SOHO fiber with $\Lambda = 2\mu m$ and $d/\Lambda = 0.81$. It can be seen that the attenuation of both fibers for which $\Lambda = 4\mu m$ and 2μm is ~5dB/m at 1.55μm, implying that as predicted, the confinement loss of the fundamental mode is negligible for these fibers and the loss is dominated by the material absorption and other factors related to the fiber fabrication process. In detail, due to the overtone of the fundamental vibration of hydrogen bonding in B1 glass, the attenuation of all the fibers increases around 1.5μm, while between 1.0-1.2μm the fibers show minimum losses of ~1.5dB/m. Additionally, due to the similar

bonding strengths of Si-O bonds and Pb-O bonds, near fiber drawing temperatures, the SiO_2-PbO glass system tends to separate into SiO_2-rich regions and PbO-rich regions at the sizes of micron or sub-micron scale [41]. Phase-separation leads to the compositional variations (and thus the index variations) within the fiber profile. Impurities in the bulk glasses are another contribution to the total fiber loss. By using high purity raw materials and melting the glasses in a dry atmosphere [54], it should ultimately be possible to reduce the total loss of this SOHO fiber at 1.55μm to below the 1dB/m level, thus opening up many practical applications for this new fiber type.

Fiber nonlinearity: One of the most attractive applications for holey fibers made from high index glasses is in nonlinear devices. In order to estimate the effective fiber nonlinearity that can be achieved in this material system, Figure 8 shows calculations of the effective mode area and corresponding fiber nonlinearity γ for a rod of material B1 surrounded by a uniform non-structured cladding of material H1. This simplified geometry represents the fundamental limit in effective mode area/nonlinearity that can be achieved in a fiber made from these two materials. The smallest mode area (and hence highest γ) occurs when the core is ~1μm in diameter. Corresponding results for a silica rod suspended in air are also shown in Figure 8. Even though the index contrast between silica/air leads to a similar mode area as the combination B1/H1, the significantly larger material nonlinearity (n_2) of material B1 results in a dramatic improvement in the nonlinearity. Hence while the maximum nonlinearity that can be achieved in a silica/air holey fiber is ~$60W^{-1}km^{-1}$, more than $500W^{-1}km^{-1}$ should ultimately be possible in a B1/H1 SOHO fiber. The Boskovic method [55] was applied to measure the effective nonlinearity of the 220μm SOHO fiber with Λ=2μm and d/Λ=0.81. Using high power dual frequency beat signals, the effective fiber nonlinearity γ was deduced from the nonlinear phase shift F_{SPM}, ($F_{SPM}=2\gamma LP$, where L is the effective fiber length and P the signal power), due to the propagation in the fiber to be $230W^{-1}km^{-1}$, which is ~200 times higher than that of standard single mode silica fiber and matches the modeled result well.

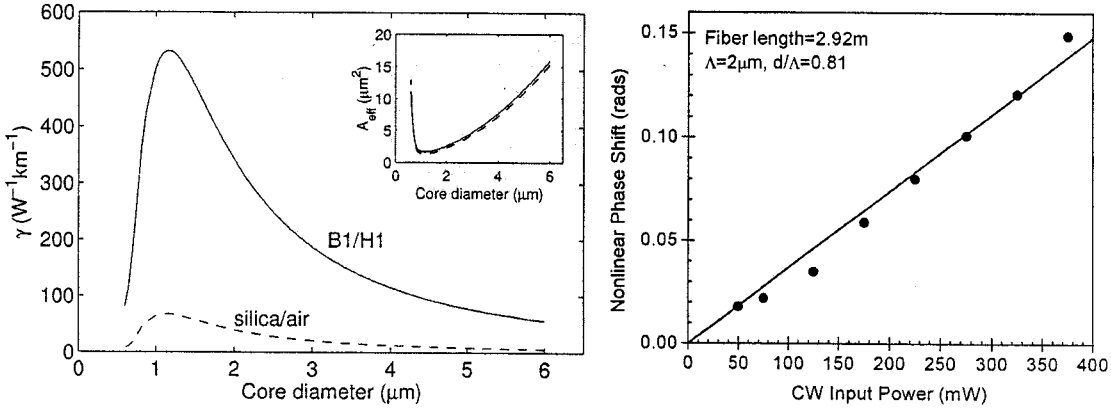

Figure 8. Effective nonlinearity of SOHO fiber (left: calculated for a range of simple step-index fiber designs, right: measured relationship between nonlinear phase shift and the input laser power at 1.55μm)

Group velocity dispersion (GVD): One of the most important applications of HFs is highly nonlinear fibers. However, the high dispersion and dispersion slope which are characteristic of many HF designs limits the useful spectral bandwidth of the fibers. In silica HFs, low and flat dispersion

can be obtained when d/Λ on the order of 0.25-0.3 with Λ=2.3μm [56,57]. Hence for the low/flat dispersion air/silica HF designs identified thus far, these GVD properties are achieved at the cost of a considerable reduction in nonlinearity relative to small core large air-fraction HFs. In contrast, the predictions in Figure 9 suggest that zero GVD in the 1.5-1.6μm wavelength range can be achieved in realistic B1/H1 SOHO fiber designs with large d/Λ and small Λ, which implies that high nonlinearity and low dispersion can be achieved simultaneously in solid-microstructured fibers.

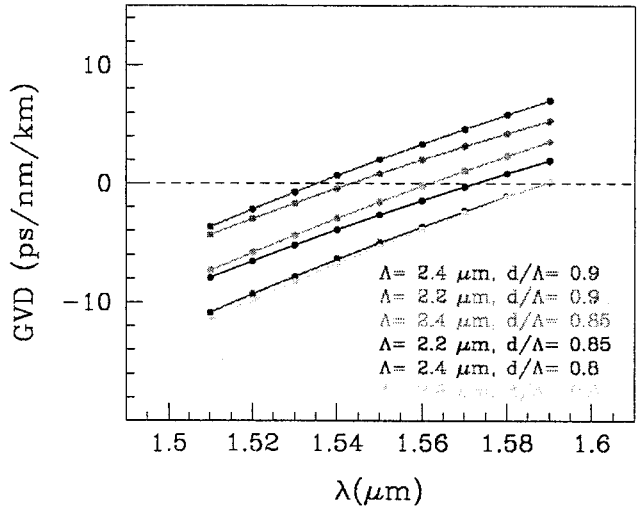

Figure 9. GVD predictions for a range of B1/H1 SOHO fibers made using a full-vector implementation of the orthogonal function method [56]. The material dispersions of B1 and H1 have been included ab initio.

Hollow core fiber with multilayered cladding

Here a brief overview of another class of solid cladding microstructured fiber: hollow core fiber with a solid multilayered photonic bandgap cladding. For more details see Reference [37]. In this work, which was conducted at MIT, a fiber designed for the transmission of 10.6μm CO_2 laser emission was producing using a combination of polymer and chalcogenide glass materials that are not themselves transparent at the operating wavelength. The periodically structured solid cladding effectively acts as a mirror for light propagating within the photonic bandgap, and light is confined to the hollow core of the fiber. The relatively low fiber losses achieved (<1dB/m) are made possible by the short penetration depths of electromagnetic waves in the high-refractive-index-contrast photonic crystal structure.

Fabrication: To achieve high index contrast in the layered portion of the fiber, a chalcogenide glass with a refractive index of 2.8 (arsenic triselenide) was combined with a high glass-transition temperature thermoplastic polymer with a refractive index of 1.55, poly(ether sulphone). These materials are thermally compatible and can be drawn into good quality layered structures. The glass layers were thermally evaporated onto a polymer film, and the coated film was rolled into a hollow multilayer tube fiber preform. This hollow macroscopic pre-form was drawn down into fiber with submicron layer thicknesses. Transmission spectra were used to confirm that the positions of the

measured transmission peaks agree with the calculated bandgaps, which confirms that light is guided in the hollow core by the photonic bandgap mechanism.

Power delivery: Using a fiber with a fundamental photonic bandgap centered near 10.6μm and a hollow core with a diameter of 700μm, CO_2 laser emission at 10.6μm was successfully transmitted. This demonstrates the substantial reduction of fiber transmission loss relative to the intrinsic loss of the constituent materials. No damage to the fibers was reported when a laser power density of $\approx 300 W/cm^2$ was coupled into the hollow fiber core. These results indicate the feasibility of using hollow multilayer photonic bandgap fibers as a transmission medium for high-power laser light in the infrared.

CONCLUSION

The synergy of novel compound glass materials and microstructured fiber technology promises a broad range of new and potentially useful optical fibers. The low softening temperatures characteristic of compound glasses allow a broad range of fabrication techniques to be exploited for the production of macroscopic fiber preforms. The technique that has been developed most extensively to date is extrusion, which has proved to be a flexible approach to realizing fibers from relatively small quantities of bulk glass. Using conventional solid fiber designs, it is in general necessary to identify two compatible glasses for the production of low loss optical fibers. Note that since microstructured fibers can be made from a single material, this technology is a powerful way of producing fibers from glasses with useful optical properties without requiring that compatible cladding materials be found.

A range of theoretical techniques have been developed in recent years to model the optical properties of silica microstructured fibers. These techniques have been applied to several non-silica microstructured fiber designs (both index-guiding and photonic bandgap). The relatively large index contrast typically found in microstructured fibers made from high index glasses makes fiber design more challenging, and in general means that it is more important to use full vectorial methods for these fibers. Numerical predictions have been used to usefully complement ongoing fabrication and experimental work for a range of index-guiding fiber designs (see for example [32]).

Using preform extrusion techniques, fibers with high effective nonlinearity have been made from a range of high-n_2 non-silica glasses. The largest reported value of effective fiber nonlinearity (γ) in a holey fiber has been realized using lead silicate glass, where $\gamma \sim 640 W^{-1}km^{-1}$ has been achieved. Theoretical work indicates that values of γ of a few thousand $W^{-1}km^{-1}$ should ultimately be possible. The best fibers of this type to date have propagation losses of approximately 3dB/m [32]. Given that this fiber type has only emerged relatively recently, it is anticipated it should be possible to reduce the losses the 1 dB/m level or below for some high n_2 glasses. Such an advance should enable this new fiber type to compete (in terms of device figure of merits) with more conventional fibers for nonlinear fiber devices. Work on improving on the design of such fib

ers as well as developing techniques that will allow more efficient coupling to conventional systems is currently under way.

The large index contrast possible in non-silica microstructured fibers is promising for the development of new fibers based on photonic bandgap effects. It has been demonstrated that increasing the refractive index contrast beyond that available in air/silica does not necessarily

broaden the photonic bandgaps that are available [58,59]. Unlike air/silica bandgap fibers, in which the photonic bandgaps widen monotonically as a function of increasing air filling fraction, the optimum air-filling fraction for high index glasses (i.e. n>2) is approximately 60% (this is referred to as type-II photonic bandgap guidance). From a practical viewpoint, this is fortuitous, since non-silica glasses tend to be relatively fragile, and it would be challenging to produce the extremely large air filling fraction designs that are typically made in air/silica structures [26]. One particularly promising application of this new fiber type will be the development of new air-guiding fibers for broadband high power IR transmission [59].

It has been demonstrated that solid microstructured fibers can be produced using a relatively small number of cladding features. Large effective nonlinearity can be combined with relatively low and flat group velocity dispersion between 1.5-1.6μm in this class of fiber. Additionally, it can be expected that the use of a solid fiber structure will lead to a number of practical advantages relative to air/glass HFs. For example, edge polishing, angle polishing and splicing should all be more straightforward in SOHO fibers [36]. Light can also be guided in air in fibers with a solid microstructured cladding [37]. In these fibers, chalcogenide/polymer cladding layers act as an interior omnidirectional dielectric mirror confining light to the hollow core via photonic bandgap effects. The transmission windows of these fibers are determined by the layer dimensions and can be scaled from 0.75 to 10.6μm in wavelength. The transmission losses are orders of magnitude lower than those of the materials used to make the fiber cladding, thus demonstrating that low attenuation can be achieved through structural design rather than high-transparency material selection.

Non-silica microstructured fibers have the potential to dramatically broaden the range of optical properties that can be offered in fiber form. For example, the combination of the high nonlinearity provided by compound glasses and the flexibility offered by microstructured fiber technology for engineering the fiber parameters should lead to the development of truly practical, low power compact nonlinear fiber devices. Solid holey fibers promise both a range of practical handling benefits and access to new optical regimes. Finally, air-core high-index photonic bandgap fibers are an attractive means to high-power transmission and new transmission windows.

REFERENCES

1. J.C. Knight, T.A. Birks, P.S.J. Russell, D.M. Atkin, "All-silica single-mode optical fiber with photonic crystal cladding", Opt. Lett. **21**, pp. 484-485, 1996
2. T.M. Monro, D.J. Richardson, "Holey optical fibres: Fundamental properties and device applications", C. R. Phys. **4**, pp. 175-186, 2003
3. P. Russell, "Photonic crystal fibers", Science **299**, pp. 358-362, 2003
4. R.F. Cregan, B.J. Mangan, J.C. Knight, T.A. Birks, P.S. J. Russell, P.J. Roberts, D.C. Allan, "Single-mode photonic band gap guidance of light in air", Nature **285**, pp.1537-1539, 1999
5. T.M. Monro, P.J. Bennett, N.G.R. Broderick, D.J. Richardson, "Holey fibers with random cladding distributions", Opt. Lett. **25**, pp. 206-208, 2000
6. T.A. Birks, J.C. Knight, P.S.J. Russell, "Endlessly single-mode photonic crystal fiber", Opt. Lett. **22**, pp. 961-963, 1997
7. J.C. Knight, J. Arriaga, T.A. Birks, A. Ortigosa-Blanch, W.J. Wadsworth, P.S.J. Russell, "Anomalous dispersion in photonic crystal fiber", IEEE Photon. Technol. Lett. **12**, pp. 807-809, 2000

8. J.C. Knight, T.A. Birks, R.F. Cregan, P.S.J. Russell, J.-P. de Sandro, "Large mode area photonic crystal fibre", Electron. Lett. **34**, pp. 1347-1348, 1998
9. B. Zsigri, C. Peucheret, M.D. Nielsen, P. Jeppesen, "Transmission over 5.6km large effective area and low-loss (1.7dB/km) photonic crystal fibre", Electron. Lett. **39**, pp. 796-798, 2003
10. P. Petropoulos, M. Monro, W. Belardi, K. Furusawa, J.H. Lee, D.J. Richardson, "2R-regenerative all-optical switch based on a highly nonlinear holey fiber", Opt. Lett. **26**, pp. 1233-1235, 2001
11. A.I. Siahlo, L.K. Oxenlowe, K.S. Berg, A.T. Clausen, P.A. Andersen, C. Peucheret, A. Tersigni, P. Jeppesen, K.P. Hansen, J.R. Folkenberg, "A high-speed demultiplexer based on a nonlinear optical loop mirror with a photonic crystal fiber", IEEE Photon. Technol. Lett. **15**, pp. 1147-1149, 2003
12. J.H. Lee, P.C. Teh, W. Belardi, M. Ibsen, T.M. Monro, D.J. Richardson, "A tunable WDM wavelength converter based on cross-phase modulation effects in normal dispersion holey fiber", IEEE Photon. Technol. Lett. **15**, pp. 437-439, 2003
13. J.E. Sharping, M. Fiorentino, P. Kumar, R.S. Windeler, "Optical parametric oscillator based on four-wave mixing in microstructure fiber", Opt. Lett. **27**, pp. 1675-1677, 2002
14. C. Peucheret, B. Zsigri, P.A. Andersen, K.S. Berg, A. Tersigni, P. Jeppesen, K.P. Hansen, M D. Nielsen, "40Gbit/s transmission over photonic crystal fibre using mid-span spectral inversion in highly nonlinear photonic crystal fibre", Electron. Lett. **39**, pp. 919-921, 2003
15. J.K. Ranka, R.S. Windeler, A.J. Stentz, "Visible continuum generation in air-silica microstructure optical fibers with anomalous dispersion at 800nm", Opt. Lett. **25**, pp. 25-27, 2000
16. P.A. Champert, S.V. Popov, J.R. Taylor, "Generation of multiwatt, broadband continua in holey fibers", Opt. Lett. **27**, pp. 122-124, 2002
17. R. Holzwarth, T. Udem, T.W. Hansch, J.C. Knight, W.J. Wadsworth, P.S.J. Russell, "Optical frequency synthesizer for precision spectroscopy", Phys. Rev. Lett. **85**, pp. 2264-2267, 2000
18. I. Hartl, X.D. Li, C. Chudoba, R.K. Ghanta, T.H. Ko, J.G. Fujimoto, J.K. Ranka, R.S. Windeler, "Ultrahigh-resolution optical coherence tomography using continuum generation in an air-silica microstructure fiber", Opt. Lett. **26**, pp. 608-610, 2001
19. W.J. Wadsworth, J.C. Knight, A. Ortigosa-Blanch, J. Arriaga, E. Silvestre, P.S.J. Russell, "Soliton effects in photonic crystal fibres at 850nm", Electron. Lett. **36**, pp. 53-55, 2000
20. B.R. Washburn, S.E. Ralph, P.A. Lacourt, J.M. Dudley, W.T. Rhodes, R.S. Windeler, S. Coen, "Tunable near-infrared femtosecond soliton generation in photonic crystal fibres", Electron. Lett. **37**, pp. 1510-1512, 2001
21. Z. Yusoff, J.H. Lee, W. Belardi, T.M. Monro, P.C. Teh, D.J. Richardson, "Raman effects in a highly nonlinear holey fiber: amplification and modulation", Opt. Lett. **27**, pp. 424-426, 2002
22. T. Hasegawa, E. Sasaoka, M. Onishi, M. Nishimura, Y. Tsuji, M. Koshiba, "Hole-assisted lightguide fiber for large anomalous dispersion and low optical loss", Opt. Express **9**, pp. 681-686, 2001
23. J.K. Sahu, C.C. Renaud, K. Furusawa, R. Selvas, J.A. Alvarez-Chavez, D.J. Richardson, J. Nilsson, "Jacketed air-clad cladding pumped ytterbium-doped fibre laser with wide tuning range", Electron. Lett. **37**, pp. 1116-1117, 2001

24. J.H.V. Price, K. Furusawa, T.M. Monro, L. Lefort, D.J. Richardson, "Tunable, femtosecond pulse source operating in the range 1.06-1.33μm based on an Yb^{3+}-doped holey fiber amplifier", J. Opt. Soc. Amer. B **19**, pp. 1286-1294, 2002
25. K. Tajima, J. Zhou, K. Kurokawa, K. Nakajima, "Low water peak photonic crystal fibres", Proc. European Conference on Optical Communication (ECOC'2003), Rimini, Italy, 2003, postdeadline paper Th4.1.6
26. Brian Mangan, Lance Farr, Allen Langford, P. John Roberts, David P. Williams, Francois Couny, Matthew Lawman, Matthew Mason, Sam Coupland, Randolf Flea, Hendrik Sabert, Tim A. Birks, Jonathan C. Knight, Philip St. J. Russell, "Low loss (1.7 dB/km) hollow core photonic bandgap fiber", PDP24 OFC'2004 (Anaheim).
27. K.M. Kiang, K. Frampton, T.M. Monro, R. Moore, J. Trucknott, D.W. Hewak, D.J. Richardson, "Extruded singlemode non-silica glass holey optical fibres", Electron. Lett. **38**, pp. 546-547, 2002
28. V.V.R.K. Kumar, A.K. George, W.H. Reeves, J.C. Knight, P.S.J. Russell, "Extruded soft glass photonic crystal fiber for ultrabroadband supercontinuum generation", Opt. Express **10**, pp. 1520-1525, 2002
29. V.V.R.K. Kumar, A.K. George, J.C. Knight, P.S.J. Russell, "Tellurite photonic crystal fiber", Opt. Express **11**, pp. 2641-2645, 2003
30. T.M. Monro, K.M. Kiang, J.H. Lee, K. Frampton, Z. Yusoff, R. Moore, J. Trucknott, D.W. Hewak, H.N. Rutt, D.J. Richardson, "High nonlinearity extruded single-mode holey optical fibers", Proc. Optical Fiber Communications Conference (OFC'2002), Anaheim, California, 2002, postdeadline paper FA1-1
31. P. Petropoulos, T.M. Monro, H. Ebendorff-Heidepriem, K. Frampton, R.C. Moore, H.N. Rutt, D.J. Richardson, "Soliton-self-frequency-shift effects and pulse compression in anomalously dispersive high nonlinearity lead silicate holey fiber", Proc. Optical Fiber Communications Cnference (OFC'2003), Atlanta, Georgia, 2003, postdeadline paper PD03
32. P. Petropoulos, H. Ebendorff-Heidepriem, V. Finazzi, R.C. Moore, K. Frampton, D.J. Richardson, T.M. Monro, "Highly nonlinear and anomalously dispersive lead silicate glass holey fibers", Opt. Express **11**, pp. 3568-3573, 2003
33. H. Ebendorff-Heidepriem, P. Petropoulos, V. Finazzi, K. Frampton, R.C. Moore, D.J. Richardson, T.M. Monro, "Highly nonlinear bismuth-oxide-based glass holey fiber, Proc. Optical Fiber Communications Conference (OFC'2004), Los Angeles, California, 2004, paper ThA4
34. P. Petropoulos, H. Ebendorff-Heidepriem, T. Kogure, K. Furusawa, V. Finazzi, T.M. Monro, D.J. Richardson, "A spliced and connectorized highly nonlinear and anomalously dispersive bismuth-oxide glass holey fiber", Proc. Conference on Lasers and Electro-Optics (CLEO'2004), San Francisco, California, 2004, paper CTuD
35. M.A. van Eijkelenborg, M.C.J. Lange, A. Argyros, J. Zagari, S. Manos, N.A. Issa, S. Fleming, R.C. McPhedran, C.M. de Sterke, N.A.P. Nicorovici, "Microstructured polymer optical fibre", Opt. Express **9**, pp. 319-327, 2001
36. X. Feng, T.M. Monro, P. Petropoulos, V. Finazzi, D.W. Hewak, "Solid microstructured optical fiber", Opt. Express **11**, pp. 2225-2230, 2003

37. Burak Temelkuran, Shandon D. Hart, Gilles Benoit, John D. Joannopoulos & Yoel Fink, "Wavelength-scalable hollow optical fibres with large photonic bandgaps for CO_2 laser transmission", Nature **420**, pp. 650-653, 2002
38. G. P. Agrawal, Nonlinear Fiber Optics (Academic Press, Boston, 2001).
39. J. H. Lee, W. Belardi, K.Furusawa, P. Petropoulos, Z.Yusoff, T.M. Monro, and D.J. Richardson, "Four-wave mixing based10-Gb/s tunable wavelength conversion using a holey fiber with a high SBS threshold," IEEE Photon. Technol. Lett. **15**, 440-442 (2003).
40. S.R. Fribergand P.W. Smith, "Nonlinear Optical-Glasses for Ultrafast Optical Switches," IEEEJ. Quantum Electron. 23, 2089-2094 (1987).
41. R.E. Slusher, J.S. Sanghera, L.B. Shaw, I.D. Aggarwal, "Nonlinear optical properties of As-Se fiber", Proceedings of OSA Topical meeting on Nonlinear Guided Waves and their Applications, Stresa, Italy, 1-4 Sep 2003
42. L. Poladian, N. A. Issa, and T. M. Monro, "Fourier decomposition algorithm for leaky modes of fibres with arbitrary geometry," Opt. Express **10**, pp. 449-454, 2002
43. E. M. Vogel, M. J. Weber, and D. M. Krol, "Nonlinear Optical Phenomena in Glass," Phys. Chem. Glasses **32**, pp. 231-254, 1991
44. S. Fujino, H. Ijiri, F. Shimizu, and K. Morinaga, "Measurement of viscosity of multi-component glasses in the wide range for fiber drawing," J. Jpn. Inst. Met. **62**, pp. 106-110, 1998
45. Schott Glass Catalogue, 2003.
46. N. Sugimoto, H. Kanbara, S. Fujiwara, K. Tanaka, Y. Shimizugawa, K. Hirao, "Third-order optical nonlinearities and their ultrafast response in Bi_2O_3-B_2O_3-SiO_2 glasses, J. Opt. Soc. Am. B **16**, pp. 1904-1908, 1999
47. K. Kikuchi, K. Taira, N. Sugimoto, "Highly nonlinear bismuth oxide-based glass fibers for all-optical signal processing", Electron. Lett. **38**, pp. 166-167, 2002
48. N. Sugimoto, Y. Kuroiwa, K. Ochiai, S. Ohara, Y. Furusawa, S. Ito, S. Tanabe, T. Hanada, "Novel short-length EDF for C+L band amplification", Proceedings of Optical Amplifiers and their Applications, Quebec City, Canada, 9-12 Jul 2000
49. Y. Kuroiwa, N. Sugimoto, K. Ochiai, S. Ohara, Y. Furusawa, S. Ito, S. Tanabe, T. Hanada, "Fusion spliceable and high efficient Bi_2O_3-based EDF for short length and broadband application pumped at 1480 nm", OFC 2001, Anaheim, California, 17-22 Mar 2001, TuI5
50. J.S. Wang, E.M. Vogel, E. Snitzer, `Tellurite glass: a new candidate for fiber devices', Opt. Mat. 3, pp. 187-203, 1994
51. R. Stegeman, L. Jankovic, H. Kim, C. Rivero, G. Tegeman, K. Richardson, P. Delfyett, Y. Guo, A. Schulte, T. Cardinal, `Tellurite glasses with peak absolute Raman gain coefficients up to 30 times that of fused silica', Opt. Lett. **28**, pp. 1126-1128, 2003
52. K. F. J. Heinrich, Electron Beam X-ray Microanalysis, (Van Nostrand Reinhold Co., 1981).
53. B. T. Kuhlmey, T. P. White, R. C. McPhedran, D. Maystre, G. Renversez, C. M. de Sterke, L. C. Botten, "Multipole method for microstructured optical fibers. II. Implementation and results," J. Opt. Soc. Am. B **19**, pp. 2331-2340, 2002
54. X. Feng, S. Tanabe, T. Hanada, "Hydroxyl groups in erbium-doped germanotellurite glasses", J. Non-Cryst. Solids **281**, pp. 48-54, 2001

55. A. Boskovic, S. V. Chernikov, J. R. Taylor, L. Gruner-Nielsen, and O. A. Levring, "Direct continuous-wave measurement of n_2 in various types of telecommunication fiber at 1.55μm," Opt. Lett. **21**, pp. 1966-1968, 1996
56. T. M. Monro, D. J. Richardson, N. G. R. Broderick, "Efficient modeling of holey fibers," Proc. Opt. Fiber Commun. Conf. No. FG3, San Diego, California 21-26 Feb 1999
57. W. H. Reeves, J. C. Knight, P.St.J. Russell, "Demonstration of ultraflattened dispersion in photonic crystal fibers", Opt. Express **10**, pp. 609-613, 2000
58. Pottage JM, Bird DM, Hedley TD, et al. "Robust photonic band gaps for hollow core guidance in PCF made from high index glass", Optics Express **11**, pp. 2854-2861, 2003
59. L.B. Shaw, J.S. Sanghera, I.D. Aggarwal, F.H. Hung, "As-S and As-Se based photonic band gap fiber for IR laser transmission", Optics Express **11**, pp. 3455-3460, 2003